International Journal of Research
Available at https://edupediapublications.org/journals
p-ISSN: 2348-6848
e-ISSN: 2348-795X
Volume 03 Issue 14
October 2016

A Single Stage CCM Micro Inverter for Solar Photovoltaic AC Module fed BLDC Applications

TIRUMANI NARESH
M-tech Scholar
Department of Electrical & Electronics Engineering,
Malla Engineering College, Dhulapally (Post. Via. Kompally),
Rangareddy (Dt); Telangana, India.
Email: tnaresh.eee@gmail.com

S. BHARATHI
Assistant Professor
Department of Electrical & Electronics Engineering,
Malla Engineering College, Dhulapally (Post. Via. Kompally),
Rangareddy (Dt); Telangana, India.
Email: barati.reddy10@gmail.com

Abstract- BRUSHLESS dc (BLDC) motors have become increasingly popular in the past decade due to the advantages such as high efficiency, high power density, compact size, high ruggedness, low maintenance requirements, and their immunity to electromagnetic interference (EMI) problems. In this theory dual-stage micro-inverters are commonly used in grid-connected photovoltaic (PV) systems. The high boost DC/DC converter is necessary for the grid-connected micro-inverter because the input voltage from a single solar panel is very small. A DC/DC Zeta converter with coupled inductor which operates at moderate duty ratios is proposed. This topology is basically derived from a conventional Zeta converter by replacing the input inductor by a coupled inductor. The turn's ratio of the coupled inductor increases the voltage gain and the secondary winding of the coupled inductor is in series with a switched capacitor for further increasing the voltage. High voltage gain is achieved by employing high turn's ratio to coupled inductor. The leakage-inductor energy of the coupled inductor is efficiently recycled to the load by additional capacitors and diodes and thus efficient energy-conversion is possible. The stress on the active switch is also restrained. The proposed Zeta converter with coupled inductor topology and BLDC is simulated and the results are obtained.

***Index Terms*— AC module, continuous conduction mode (CCM), micro inverter, photovoltaic (PV), zeta**

I INTRODUCTION

To address the growing concern of depletion of fossil fuels, energy cost, and CO2 emission, higher penetration of renewable energy sources into the grid is encouraged. Among various renewable energy sources, solar is the most abundant form of energy. Series connected photovoltaic (PV) panels with a single large inverter (string inverter) can be used to feed power into the grid with a common maximum power point tracking (MPPT). However, this is an inefficient way of harvesting energy because individual MPPT of solar panels is not achieved. A panel mismatch, shading, or formation of debris will reduce the energy harvest significantly. To solve the above-mentioned problem, the concept of micro inverter is picking up. Micro inverters are attached at the back of a PV panel and directly generate ac with MPPT [1]–[3]. Improving the efficiency, reducing number of power conversion stages, and scalability are major design considerations.

Among various micro inverters reported in the literature, the most generic is two stage inverters where a dc/dc converter is used in the front end to track MPPT and to boost the voltage, while the second-stage pulse width modulated inverter convert dc to ac [4]. The major drawback of this type of inverters is the components count and cost. No isolated micro inverters are simple and compact, but boosting the voltage to the grid level without transformer is a major concern [10]. Third kind is single-stage micro inverters where all three tasks, i.e., MPPT, voltage boosting, and dc to ac conversion are done in one stage. Such micro inverters are very promising due to reduced switch count and high power density [14]. Other types of micro inverters utilize active power decoupling that enables the use of thin-film capacitors instead of electrolytic capacitors to increase the life span of the micro inverter. However, this comes with an additional cost and relatively low efficiency [16].

Among single-stage micro inverters, fly back converter with a line frequency inverter (LFI) is the most commonly reported topology as there is only one main switch on the primary. Most of the fly back inverters reported in the literature operate under discontinuous conduction mode (DCM). The DCM mode of operation leads to higher inverter losses, current stress, and component rating compared to CCM operation [20]–[23]. This is due to the control complexity\ caused by the right half plan (RHP) zero when fly back converter is operated in the CCM. To address the problems in fly back inverter and to achieve CCM operation with a moving RHP zero, Yanlin and Oruganti proposed control strategies and demonstrated significant efficiency improvement. However, designing controller with a moving RHP zero is always a challenge.

Modeling of zeta dc/dc converter and parameter selection to eliminate RHP zero was earlier reported in It is concluded that zeta converter can achieve higher bandwidth and good closed-loop stability. A DCM mode zeta converter-based inverter was earlier reported in. The inverter power rating was limited to 80 W. Low switching frequency (20 kHz) operation resulted into a larger filter and transformer. In this paper, a novel single-stage CCM zeta micro inverter is proposed as shown in Fig. 1, with a single

International Journal of Research
Available at https://edupediapublications.org/journals
p-ISSN: 2348-6848
e-ISSN: 2348-795X
Volume 03 Issue 14
October 2016

primary switch and four secondary switches working as LFI. The objectives and layout of this paper are as follows. Steady-state operation and analysis of zeta micro inverter are

II PROPOSED TOPOLOGY AND DETAILED ANALYSIS OF CCM ZETA MICROINVERTER

This section studies the steady-state operation of the proposed micro inverter. To simplify analysis, the following

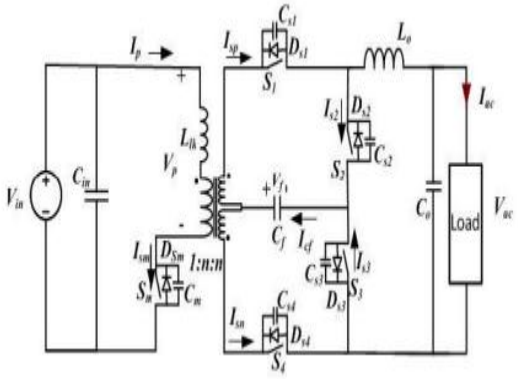

Fig.1.Proposed zeta micro inverter

Assumptions are made:

1) All semiconductor devices are ideal and lossless and

2) Input voltage ripple is negligible.

Operation of zeta micro inverter is explained for the positive half cycle of load current at switching frequency. The main switch *Sm* is modulated at high frequency (HF) with a variable duty cycle to generate rectified ac output and the secondary switches *S*1–*S*4 are operated at line frequency to produce ac output at line frequency. On the secondary side, during positive half cycle of load current switches *S*1 and *S*3 are gated to conduct and during negative half cycle of load current, switches *S*2 and *S*4 are gated to conduct. Steady-state operation of the proposed micro inverter in DCM and CCM mode of operation is analyzed. Equivalent circuits for the inverter in different operating modes are shown in Fig. 2. Steady-state operating waveforms of zeta micro inverter in DCM and CCM modes are shown in Figs. 3 and 4, respectively.

A. DCM Mode of Operation

1) Interval 1 (td0 < t < td1) Fig. 2(a): At *t* = *td*0, the main switch *Sm* is turned-ON. Secondary switches *S*1 and *S*3 are conducting for the entire positive half cycle of load current. Diode *Ds*2 is reverse biased as shown in Fig. 2(a). Primary current *Ip*increases linearly starting from zero as shown in Fig. 3. Primary current *Ip*and magnetizing inductor current *Ilm*can be given as

$$i_p(t) = \left(\frac{V_{\text{in}}}{L_m} + \frac{n^2 V_{\text{in}}}{L_o}\right)(t - t_{d0}) \tag{1}$$

$$i_{lm}(t) = I_{lm}(t_{d0}) + \left(\frac{V_{\text{in}}}{L_m}\right)(t - t_{d0}). \tag{2}$$

In this interval, secondary switch current *is*2 = 0 and secondary side currents *isp*, *iLo*, and *icf*are similar due to series connection as shown in Fig. 2(a) and the values are derived as

$$i_{sp}(t) = \frac{i_p(t) - i_{lm}(t)}{n} = i_{Lo}(t) = -i_{cf}(t). \tag{3}$$

Flying capacitor *C f* is discharging, and at the end of this interval, its voltage falls below the minimum value, *Vcf*_ min.

At the end of this interval, primary current *ip* reaches maximum value denoted by *Ip*_peakgiven by (4). Duration of this interval is equal to *DTs* (*td*1 = *DTs*) where *D* is the

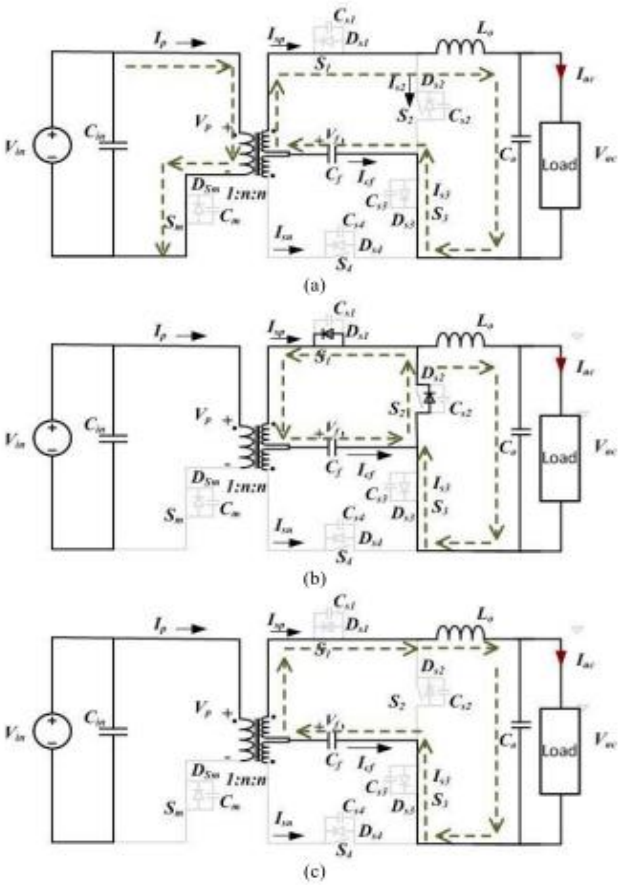

Fig. 2. Equivalent circuit depicting the different intervals of operation of the proposed micro inverter, (a) Interval 1, (b) Interval 2 and (c) Interval 3

duty cycle and *Ts*is the time period of main switch *Sm*

$$I_p(t_{d1}) = I_{p\_peak} = \left(\frac{V_{in}}{L_m} + \frac{n^2 V_{in}}{L_o}\right)(DT_s) \quad (4)$$

$$I_{Lo}(t_{d1}) = I_{Lo\_peak} = \frac{I_{p\_peak} - I_{Lm}(t = t_{d1})}{n}. \quad (5)$$

2) Interval 2 (td1 < t < td2) Fig. 2(b): At *t* = *td*1, the main switch *Sm* is turned-OFF and secondary side diode *Ds*2 goes into conduction. At the start of this interval, the diode current is equal to peak primary current *Ip*_peakreferred to secondary given by

$$I_{ds2}(t_{d1}) = -I_{s2}(t_{d1}) = \frac{I_{p\_peak}}{n} \quad (6)$$

$$I_{s2}(t_{d1}) = -\frac{I_{p\_peak}}{n} = -\frac{\left(\frac{V_{in}}{L_m} + \frac{n^2 V_{in}}{L_o}\right)(DT_s)}{n}. \quad (7)$$

The magnetizing inductance *L M* starts charging the flying capacitor from initial value of *Vc f* _ min. Switch current *is*2 and

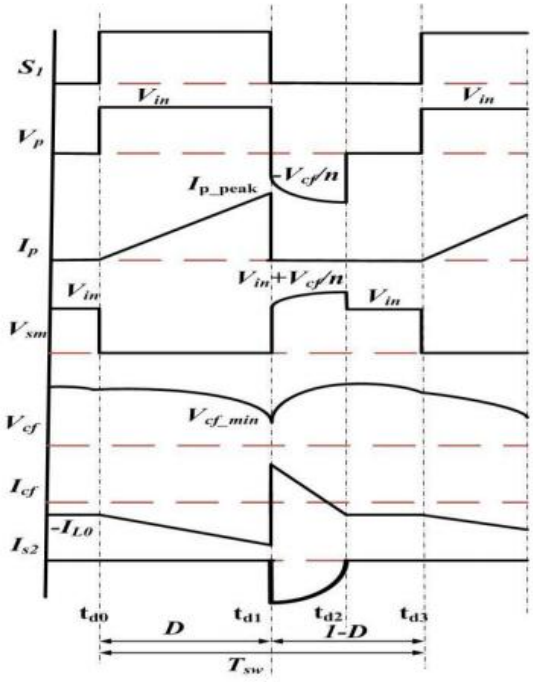

Fig.3. Steady-state operating waveforms of for proposed inverter in DCM mode of operation output inductor current *iLo* are given as

$$i_{s2}(t) = -\frac{I_{p\_peak}}{n} + \frac{V_o}{L_o}(t - t_{d1}) + \frac{v_{cf}(t)}{n^2 L_m}(t - t_{d1}) \quad (8)$$

$$v_{cf}(t) = V_{cf\_min} + \frac{1}{C_f}\int i_{cf}\,dt \quad (9)$$

$$i_{Lo}(t) = I_{Lo\_peak} - \frac{V_0}{L_0}(t - t_{d1}). \quad (10)$$

It should be noted from (9) that with increase in value of flying capacitor, voltage ripple will reduce. Average voltage across the output capacitor and the flying capacitor is equal for given switching cycle (*Vcf* = *Vo)*. Thus, for higher values of flying capacitance, *vcf*is approximately equal to the output voltage *Vo* and is constant for a given switching cycle.

Therefore, the switch current *is*2 can be approximated to

$$i_{s2}(t) = -\frac{I_{p\_peak}}{n} + \frac{V_o}{L_o}(t - t_{d1}) + \frac{V_o}{n^2 L_m}(t - t_{d1}). \quad (11)$$

However, for a practical design with higher flying capacitance value, corresponding increase in equivalent series resistance (ESR) of capacitor will increase conduction losses. Although, conduction losses in the diode *Ds*2 will reduce with increasing capacitance value. Thus, an optimum value of the flying capacitor should be chosen to limit overall losses. This interval ends when the switch current *is*2 becomes zero. Thus, duration of this interval can be obtained by making *is*2 = 0, and substituting *t* = *td*2 which is given by

$$t_{d2} = \frac{\frac{I_{p\_peak}}{n} + \left(\frac{V_0}{L_0} + \frac{V_o}{n^2 L_m}\right)(DT_s)}{\left(\frac{V_0}{L_0} + \frac{V_o}{n^2 L_m}\right)}. \quad (12)$$

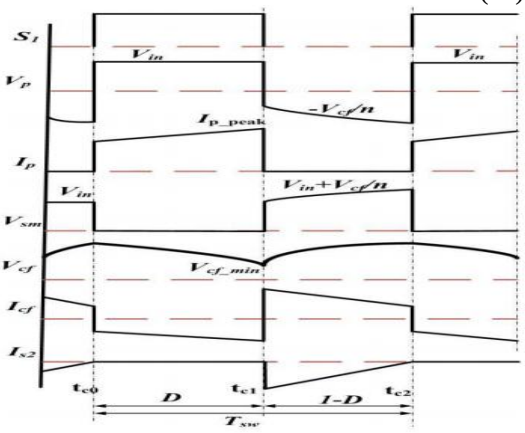

Fig.4.Steady-state operating waveforms of the proposed inverter in CCM mode of operation

At the end of this interval, inductor current *iLo* is given by

$$I_{Lo}(t_{d2}) = I_{Lo\_peak} - \frac{V_o}{L_o}(t_{d2} - DT_s).$$

(13)

3) Interval 3 (td2 < t < td3) Fig. 2(c): This interval starts when the secondary diode current *is*2 becomes zero and extends until the primary switch is turned-ONat *t* = *td*3. This interval is seen only if inverter goes into DCM and equivalent circuit for this time interval is shown in Fig. 2(c). A voltage (*Vcf–Vo)* appears across the output inductor and its current expression is

$$i_{Lo}(t) = I_{Lo}(t_{d2}) + \frac{V_{cf} - V_o}{L_o}(t - t_{d2}).$$

(14)

The second term in (14) is very small which makes inductor current approximately dc. The same current flows through the magnetizing inductance but negative. At the end of this interval, the current *iLo* and *ilm*are given by

$$I_{Lo}(T_s) = I_{Lo}(t_{d2}) + \frac{V_{cf} - V_o}{L_o}(T_s - t_{d2})$$

(15)

$$I_{lm}(T_s) = I_{lm}(t_{d0}) = -nI_{Lo}(T_s).$$

(16)

The inverter operation is repeated at switching frequency with a variable duty cycle *D* to generate a rectified sine output. Once the reference load current is negative, switches *S*1 and *S*3 are turned-OFF, and the switches *S*2, *S*4 are turned-ON.

B. CCM Mode of Operation:

1) Interval 1 (tc0 < t < tc1) Fig. 2(a): At *t* = *tc*0, the main switch *Sm* is turned-ONand secondary switches *S*1, *S*3 are conducting throughout the positive half cycle. Equivalent circuit of the proposed zeta inverter for this interval is shown in Fig. 2(a). Fig. 4 shows the steady-state operating waveforms when operated in CCM. This interval is common to both DCM and CCM but prior to this interval the voltage across the primary of the transformer is nonzero, thus the current in the primary starts from a minimum value. In this interval input voltage, *V*in is applied across the magnetizing inductance *Lm* of the transformer. Diode *Ds*2 is reverse biased, thus the secondary switch current *is*2 = 0 in this interval. Mathematical equations for the various current waveforms are

$$i_p(t) = I_p(t_{c0}) + \left(\frac{V_{\text{in}}}{L_m} + \frac{n^2 V_{\text{in}}}{L_o}\right)(t - t_{c0})$$

(17)

$$i_{lm}(t) = I_{lm}(t_{c0}) + \left(\frac{V_{\text{in}}}{L_m}\right)(t - t_{c0})$$

(18)

$$i_{sp}(t) = \frac{i_p(t) - i_{lm}(t)}{n} = i_{Lo}(t) = i_{cf}(t).$$

(19)

At the end of this interval, flying capacitor is discharged to *Vcf*_ min, currents *Ip*, *ILm*, and *ILo*reach their peak values which can be represented by *Ip*_peak, *ILm*_peak, and *ILo*_peak, respectively, and are given by

$$I_p(t_{c1}) = I_{p\_peak} = I_p(t_{c0}) + \left(\frac{V_{\text{in}}}{L_m} + \frac{n^2 V_{\text{in}}}{L_o}\right)(DT_s)$$

(20)

$$I_{Lm}(t_{c1}) = I_{Lm\_peak} = I_{Lm}(t_{c0}) + \left(\frac{V_{\text{in}}}{L_m}\right)(DT_s)$$

(21)

$$I_{Lo}(t_{c1}) = I_{Lo\_peak} = \frac{I_{p\_peak} - I_{Lm\_peak}}{n}.$$

(22)

This interval with duration *DTs* ends when the main switch *Sm*is turned-OFF.

2) Interval 2 (tc1 < t < tc2) Fig. 2(b): At *t* = *tc*1 the main switch *Sm* is turned-OFF and secondary side diode *Ds*2 goes into conduction as shown in Fig. 2(b). At the start of this interval, the diode current is equal to peak primary current *Ip*_peakreferred to secondary, which can be given as

$$I_{ds2}(t_{c1}) = -I_{s2}(t_{c1}) = \frac{I_{p\_peak}}{n}$$

(23)

$$I_{s2}(t_{c1}) = -\frac{I_{p\_peak}}{n} = -\frac{I_p(t_{c0}) + \left(\frac{V_{\text{in}}}{L_m} + \frac{n^2 V_{\text{in}}}{L_o}\right)(DT_s)}{n}.$$

(24)

Output voltage of −*Vo* is applied across the inductor *Lo* and the inductor current decreases linearly given by

$$i_{Lo}(t) = I_{Lo\_peak} - \frac{V_o}{L_o}(t - DTs).$$

(25)

Flying capacitor voltage *VC f* appears across the magnetizing inductance, but the average voltage across the output capacitor and the flying capacitor is equal for given switching cycle (*Vc f* = *Vo*). Thus, for higher values of flying capacitance, *vcf*is approximately equal to the output voltage *V*0 and the current in flying capacitor *Ic f* increases linearly with

a slope Vo/*(n*2*Lm)* thus the expression for switch current can be given as

$$i_{s2}(t) = -\frac{I_{p\_peak}}{n} + \frac{V_0}{L_0}(t - t_{c1}) + \frac{V_0}{n^2 L_m}(t - t_{c1}).$$

(26)

For CCM operation, switch *Sm* is turned-ONbefore the diode current reaches zero. Thus, the currents at the end of this interval are equal to currents at the start of the next interval

$$I_p(t = t_{c0}) = -n(I_{s2}(T_s))$$

(27)

$$I_{Lm}(t = t_{c0}) = n(I_{cf}(T_s)).$$

(28)

Substituting (26) in (27), the expression for the initial current when the primary switch is turned-ONcan be obtained as

$$I_p(t_{c0}) = n\left(\frac{I_{p\_peak}}{n} - (1 - DT_s)\left(\frac{V_0}{L_0} + \frac{V_0}{n^2 L_m}\right)\right).$$

(29)

From the above analysis, it should be realized that CCM operation of zeta micro inverter results into lower rms to average current ratio compared with DCM mode as the current ripple in the inductors *L M* and *Lo* are reduced. This will in turn translate into improved inverter efficiency as the conduction losses are reduced.

III BLDC MOTOR

BLDC engine comprises of the perpetual magnet rotor and an injury stator. The brushless engines are controlled utilizing a three stage inverter. The engine obliges a rotor position sensor for beginning and for giving legitimate compensation arrangement to turn on the force gadgets in the inverter extension. In light of the rotor position, the force gadgets are commutated consecutively every 60 degrees. The electronic compensation takes out the issues connected with the brush and the commutator plan, in particular starting and destroying of the commutator brush course of action, along these lines, making a BLDC engine more rough contrasted with a dc engine. Fig.4 demonstrates the stator of the BLDC engine and fig.5 shows rotor magnet plans.

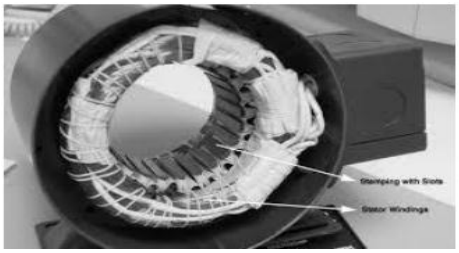

Fig.5. BLDC motor stator construction

Fig.6. BLDC motor Rotor construction.

The brush less dc engine comprise of four fundamental parts Power converter, changeless magnet brushless DC Motor (BLDCM), sensors and control calculation. The force converter changes power from the source to the BLDCM which thus changes over electrical vitality to mechanical vitality. One of the remarkable highlights of the brush less dc engine is the rotor position sensors, in view of the rotor position and order signals which may be a torque charge, voltage summon, rate order etc; the control calculation s focus the entryway sign to every semiconductor in the force electronic converter.

The structure of the control calculations decides the sort of the brush less dc engine of which there are two principle classes voltage source based drives and current source based drives. Both voltage source and current source based commute utilized for perpetual magnet brushless DC machine. The back emf waveform of the engine is demonstrated in the fig. 6. Be that as it may, machine with a non sinusoidal back emf brings about diminishment in the inverter size and lessens misfortunes for the same influence level.

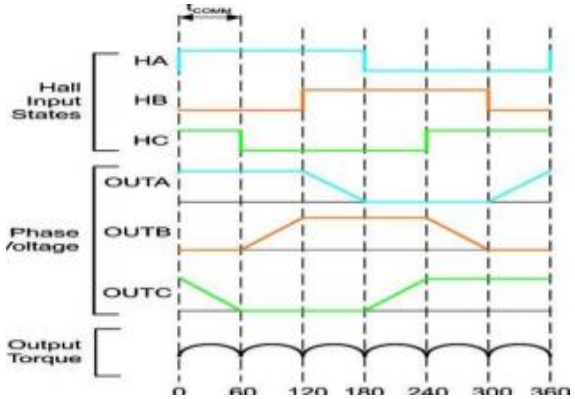

Fig.7. Hall signals & Stator voltages.

IV MATLAB/SIMULATION RESULTS

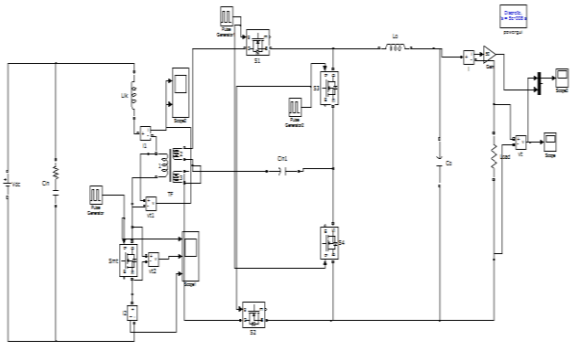

Fig 8 .Matlab/simulation circuit of proposed zeta micro inverter

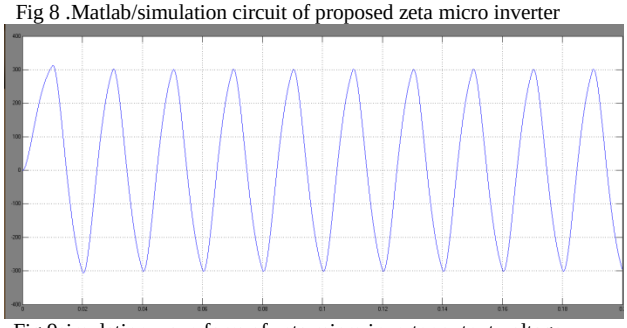

Fig 9simulation wave form of zeta micro inverter output voltage

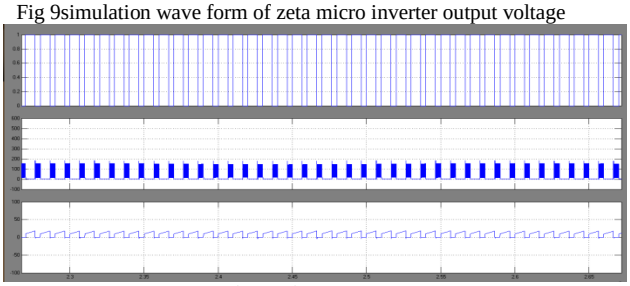

Fig 10 simulation wave form of Zeta micro inverter switching voltage

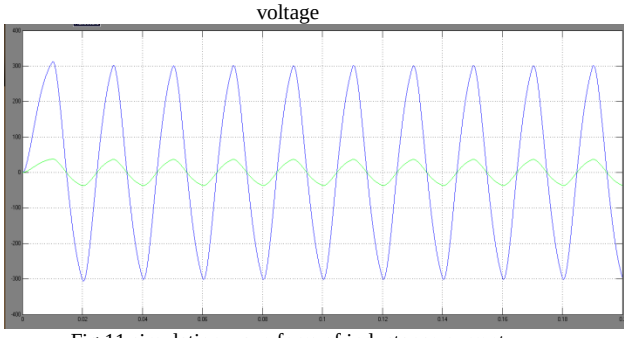

Fig 11 simulation wave form of inductance current

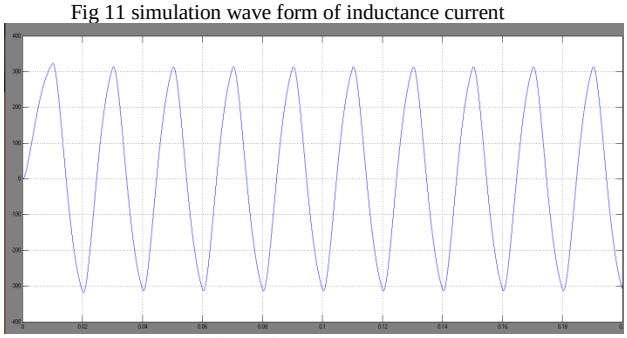

Fig 12 simulation wave form of zeta micro inverter output voltage at different load condition

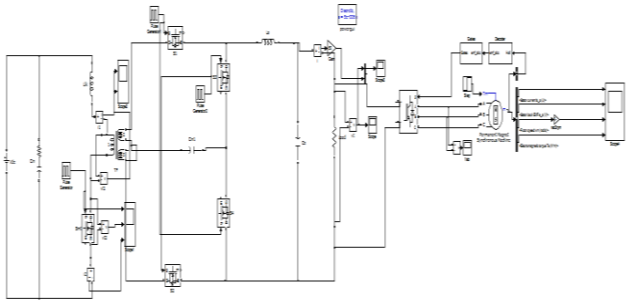

Fig 13 Matlab/simulation circuit of proposed zeta micro inverter with BLDC motor drive

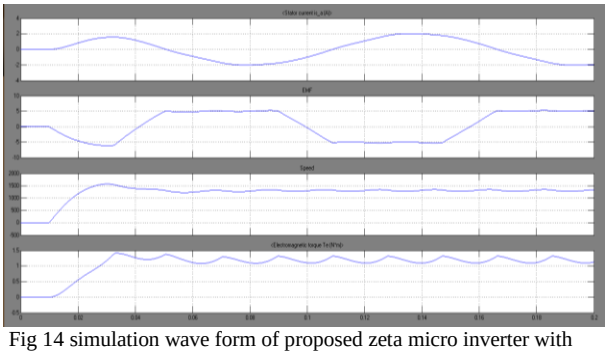

Fig 14 simulation wave form of proposed zeta micro inverter with BLDC motor drive stator current, EMF, speed and torque

V CONCLUSION:

A single-stage novel CCM zeta micro inverter has been proposed for solar PVAC module. Steady-state operation and analysis of the proposed zeta micro inverter in both DCM and CCM have been studied. Micro inverter operation in CCM mode results in reduced conduction losses, switch ratings, and current stress. The traditional CCM mode fly back inverters have closed-loop complexity and stability issues. The proposed inverter provides HF isolation and has only a single switch operating at HF which will reduce the switching losses. The circuit is simple and easy to develop. Critical factors to consider while designing the inverter have been discussed and studied. A 220-W inverter prototype has been developed and tested in the laboratory to validate the claims, proposed operation, and design. The laboratory prototype has a peak efficiency of 93% at rated power of 220 W is connected to BLDC motor and study the characteristics of BLDC motor

REFERENCES:

[1] S. B. Kjaer, J. K. Pedersen, and F. Blaabjerg, "A review of single-phase grid-connected inverters for photovoltaic modules," IEEE Trans. Ind. Appl., vol. 41, no. 5, pp. 1292–1306, Sep./Oct. 2005.
[2] J. M. Carrasco et al., "Power-electronic systems for the grid integration of renewable energy sources: A survey," IEEE Trans. Ind. Electron., vol. 53, no. 4, pp. 1002–1016, Jun. 2006.
[3] Q. Li and P. Wolfs, "A review of the single phase photovoltaic module integrated converter topologies with three different DC link configurations," IEEE

Trans. Power Electron., vol. 23, no. 3, pp. 1320–1333, May 2008.
[4] Q. Li and P. Wolfs, "A current fed two-inductor boost converter with an integrated magnetic structure and passive lossless snubbers for photovoltaic module integrated converter applications," IEEE Trans. Power Electron., vol. 22, no. 1, pp. 309–321, Jan. 2007.
[5] C. Rodriguez and G. Amaratunga, "Long-lifetime power inverter for photovoltaic AC modules," IEEE Trans. Ind. Electron., vol. 55, no. 7, pp. 2593–2601, Jul. 2008.
[6] B. Liu, S. Duan, and T. Cai, "Photovoltaic DC-building-module-based BIPV system—Concept and design considerations," IEEE Trans. Power Electron., vol. 26, no. 5, pp. 1418–1429, May 2011.
[7] S. Jiang, D. Cao, Y. Li, and F. Z. Peng, "Grid-connected boost-halfbridge photovoltaic microinverter system using repetitive current control and maximum power point tracking," IEEE Trans. *Power Electron.*, vol. 27, no. 11, pp. 4711–4722, Nov. 2012.
[8] W.-Y. Choi, "High-efficiency DC–DC converter with fast dynamic response for low-voltage photovoltaic sources," *IEEE Trans. PowerElectron.*, vol. 28, no. 2, pp. 706–716, Feb. 2013.
[9] D. R. Nayanasiri, D. M. Vilathgamuwa, and D. L. Maskell, "Half-wave cycloconverter-based photovoltaic microinverter topology with phaseshift power modulation," *IEEE Trans. Power Electron.*, vol. 28, no. 6, pp. 2700–2710, Jun. 2013.
[10] Y. Chen and K. M. Smedley, "A cost-effective single-stage inverter with maximum power point tracking," *IEEE Trans. Power Electron.*, vol. 19, no. 5, pp. 1289–1294, Sep. 2004.
[11] H. Patel and V. Agarwal, "A single-stage single-phase transformer-less doubly grounded grid-connected PV interface," *IEEE Trans. EnergyConvers.*, vol. 24, no. 1, pp. 93–101, Mar. 2009.
[12] W. Yu *et al.*, "High-efficiency inverter with H6-type configuration for photovoltaic non-isolated ac module applications," in *Proc. 25th Annu.IEEE Appl. Power Electron. Conf. Expo. (APEC)*, Palm Springs, CA, USA, Feb. 2010, pp. 1056–1061.
[13] B. Yang, W. Li, Y. Gu, W. Cui, and X. He, "Improved transformerless inverter with common-mode leakage current elimination for a photovoltaic grid-connected power system," *IEEE Trans. Power Electron.*, vol. 27, no. 2, pp. 752–762, Feb. 2012.
[14] Y.-K. Lo and J.-Y. Lin, "Active-clamping ZVS flyback converter employing two transformers," *IEEE Trans. Power Electron.*, vol. 22, no. 6, pp. 2416–2423, Nov. 2007.
[15] Y.-C. Hsieh, M.-R. Chen, and H.-L. Cheng, "An interleaved fly back converter featured with zero-voltage transition," *IEEE Trans. PowerElectron.*, vol. 26, no. 1, pp. 79–84, Jan. 2011.
[16] T. Shimizu, K. Wada, and N. Nakamura, "Flyback-type single-phase utility interactive inverter with power pulsation decoupling on the DC input for an AC photovoltaic module system," *IEEE Trans. PowerElectron.*, vol. 21, no. 5, pp. 1264–1272, Sep. 2006.
[17] F. Shinjo, K. Wada, and T. Shimizu, "A single-phase grid-connected inverter with a power decoupling function," in *Proc. IEEE PowerElectron. Specialists Conf. (PESC)*, Jun. 2007, pp. 1245–1249.
[18] H. Hu *et al.*, "A three-port flyback for PV microinverter applications with power pulsation decoupling capability," *IEEE Trans. Power Electron.*, vol. 27, no. 9, pp. 3953–3964, Sep. 2012.
[19] H. Hu, S. Harb, N. H. Kutkut, Z. J. Shen, and I. Batarseh, "A single-stage microinverter without using eletrolytic capacitors," *IEEETrans. Power Electron.*, vol. 28, no. 6, pp. 2677–2687, Jun. 2013.
[20] A. C. Kyritsis, E. C. Tatakis, and N. P. Papanikolaou, "Optimum design of the current-source flyback inverter for decentralized grid-connected photovoltaic systems," *IEEE Trans. Energy Convers.*, vol. 23, no. 1, pp. 281–293, Mar. 2008.
[21] Y. Li and R. Oruganti, "A low cost flyback CCM inverter for AC module application," *IEEE Trans. Power Electron.*, vol. 27, no. 3, pp. 1295–1303, Mar. 2012.
[22] Y.-H. Kim, Y.-H. Ji, J.-G. Kim, Y.-C. Jung, and C.-Y. Won, "A new control strategy for improving weighted efficiency in photovoltaic AC module-type interleaved flyback inverters," *IEEE Trans. PowerElectron.*, vol. 28, no. 6, pp. 2688–2699, Jun. 2013.
[23] F. F. Edwin, W. Xiao, and V. Khadkikar, "Dynamic modeling and control of interleaved flyback module-integrated converter for PV power applications," *IEEE Trans. Ind. Electron.*, vol. 61, no. 3, pp. 1377–1388, Mar. 2014.
[24] E. Vuthchhay and C. Bunlaksananusorn, "Modeling and control of a Zeta converter," in *Proc. Power Electron. Conf. (IPEC)*, Jun. 2010, pp. 612–619.
[25] R. C. Viero, H. F. M. Lopez, C. A. Zollmann, and F. S. dos Reis, "Dynamic modeling of a sinusoidal inverter based on ZETA converter working in DCM for PV arrays," in *Proc. 36th Annu. Conf. IEEE Ind.Electron. Soc. (IECON)*, Nov. 2010, pp.439–444.